Encapsulated Silicon Nanocrystals Formed in Silica by Ion Beam Synthesis

Han-Woo Choi,* Hyung-Joo Woo, Joon-Kon Kim, Gi-Dong Kim, Wan Hong, and Young-Yong Ji

Korean Institute of Geoscience and Mineral Resources, Daejeon 305-350, Korea
Received October 8, 2003

The photoluminescence (PL) emission of Si nanocrystals synthesized by 400 keV Si ion implanted in SiO_2 is studied as a function of ion dose and annealing time. The formation of nanocrystals at around 600 nm from the surface was confirmed by RBS and HRTEM, and the Si nanocrystals showed a wide and very intense PL emission at 700-900 nm. The intensity of this emission showed a typical behaviour with a fast transitory increase to reach a saturation with the annealing time, however, the red shift increased continuously because of the Ostwald ripening. The oversaturation of dose derived a decrease of PL intensity because of the diminishment of quantum confinement. A strong enhancement of PL intensity by H passivation was confirmed also, and the possible mechanism is discussed.

Key Words : Silicon, Nanocrystal, Photoluminescence, Passivation

Introduction

Bulk Si crystal does not emit photoluminescence because of its indirect band gap. But strong visible photoluminescence is observed from Si nanocrystals in SiO_2.[1-7] So they are potential candidates for Si compatible light emitting devices. Si nanocrystals can be fabricated by several methods. Ion implantation method is one of the most versatile methods. Implantation of Si builds up excess Si in a matrix, and subsequent thermal annealing forms Si nanocrystal by precipitation. This technique can form nanocrystals in mechanically robust and chemically stable matrix. And it allows for some control over nanocrystal size, distribution and depth. It also has disadvantages: energetic ions produce radiation damage in silica, and the Gaussian concentration profile produced by implantation results in a broad size distribution for Si crystallites. But the defect-related luminescence[1] can be reduced by subsequent annealing.

Light emission is known to be associated with the presence of Si nanocrystals, but its origin remains controversial.[8-10] Recombination of excitons within the nanocrystal itself[1,10,11] and defect recombination in the Si-SiO_2 interface[12-15] are pleaded as the origin of light emission. Additional annealing in hydrogen-rich environment enhances the photoluminescence from nanocrystals because of the passivation of non-radiative defects by the hydrogen.[16-18]

In this study, the formation of nanocrystals was verified by TEM and RBS. And photoluminescence of Si nanocrystals along to various Si doses and annealing conditions was measured to study the optical property of Si nanocrystals. Hydrogen passivation effect on the PL intensity enhancement was studied as well.

Experiments

400 keV Si^+ ions were implanted on 0.4 mm thick fused silica plates (Sanwa, Japan) at room temperature. Electron supply system was used to eliminate the damage caused by the charging effect of insulator samples during implantation. The implanted doses were varied from 2.0×10^{16} Si/cm^2 to 4.0×10^{17} Si/cm^2. The depth profile of Si was simulated by Srim2003 code and measured by RBS analysis. The implanted samples were annealed at 1100 ^oC in Ar environment to form Si nanocrystals, and the annealing times were varied from 1 minute to 8 hours. The samples annealed at 1100 ^oC for 2 hours were annealed once more at 500 ^oC for 1 hours in Ar + 4% H_2 forming gas to verify the enhancement of PL intensity by hydrogen passivation.

Cross-sectional HRTEM (CM-200, Philips) was used to verify the size, distribution and crystality of Si nanocrystals. Photoluminescence spectra were collected at room temperature with 250 mW 488 nm Ar laser, a grating spectrometer and GaAs photomultiplier tube. And standard lock-in detection techniques were used to enhance the signal-to-noise ratio.

Results and Discussion

RBS analysis. Figure 1 shows the profile of Si concen-

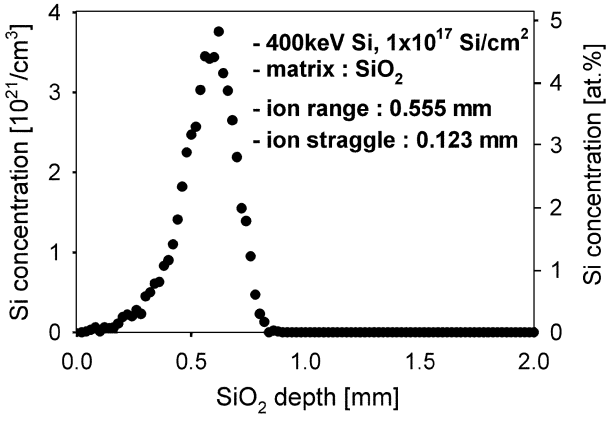

Figure 1. Estimated depth profile of 400 keV Si ions simulated with Srim2003.

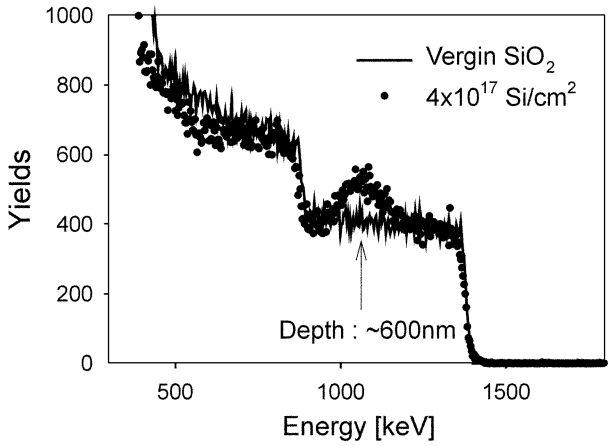

Figure 2. RBS spectra of 400 keV Si implanted SiO_2 and virgin SiO_2.

tration simulated by Srim2003 code. It has a peak near 550 nm with 250 nm FWHM. The 4.0×10^{17} Si/cm^2 dose implanted sample was analysed by RBS, and it shows excess Si peak near 600 nm in Figure 2. The Si concentration at the peak is measured to be about 45 at.% (concentration of excess Si = 17.5 at.%) by RBS, which agrees well with the simulation result.

HRTEM analysis. A 200 keV HRTEM was performed on the samples implanted with 2×10^{17} Si/cm^2 and 4×10^{17} Si/cm^2 doses and annealed for 4 hours at 1100 °C. A cross-sectional TEM image of 4×10^{17} Si/cm^2 implanted sample is shown in Figure 3, which confirms the formation of nanocrystals. The distributions of nanocrystal size were measured from this image, and the mean size of nanocrystals was 3.1 nm with 2×10^{17} Si/cm^2 dose and 5.2 nm with 4×10^{17} Si/cm^2 dose as shown in Figure 4. The size of Si nanocrystal increased and the profile of size broadened as the dose of implanted Si increased.

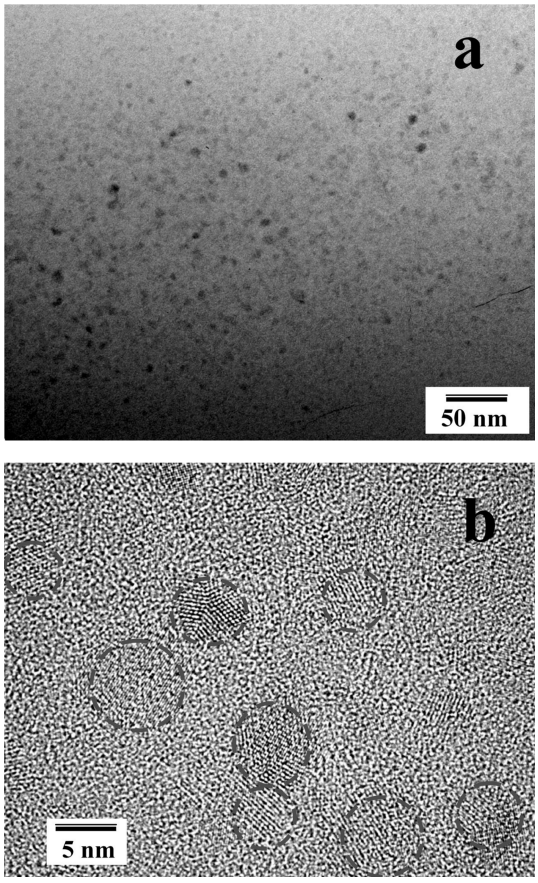

Figure 3. Spatial distribution of Si nanocrystals imaged by HRTEM for the sample implanted with 4×10^{17} Si/cm^2 dose and annealed at 1100 °C for 4 h.

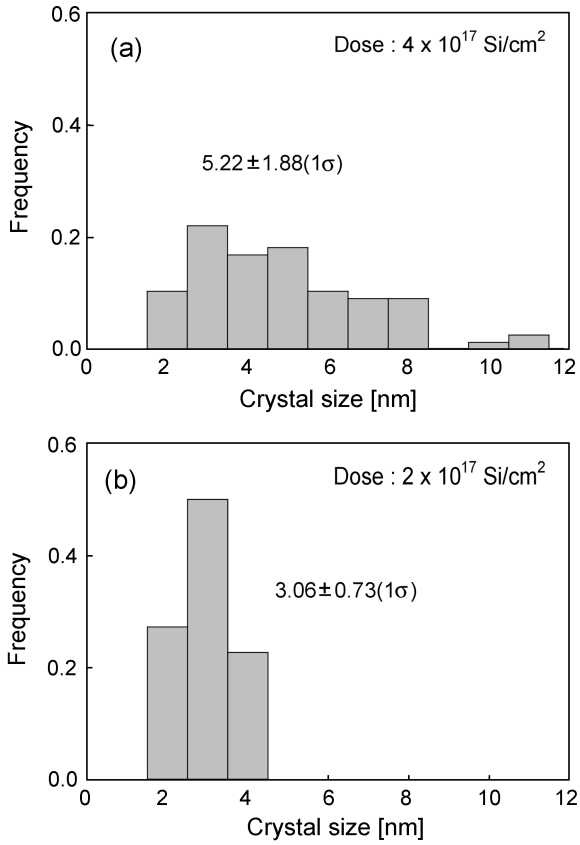

Figure 4. Size distributions of Si nanocrystals implanted with (a) 4×10^{17} Si/cm^2 and (b) 2×10^{17} Si/cm^2 doses and annealed at 1100 for 4 h.

Photoluminescence. Annealing times were varied from 1 minute to 8 hours. The PL spectra of the samples implanted at 2×10^{16} Si/cm^2 and 2×10^{17} Si/cm^2 are shown in Figure 5. In the as-implanted state, photoluminescence centered at around 650 nm was observed which was diminished remarkably within 1 minute annealing. It is believed to arise from defects introduced into the SiO_2 matrix during the implantation procedure and to be eliminated with annealing.[19] Annealing at 1100 °C gave rise to the formation of Si nanocrystal, and strong PL peaked at around 800 nm was observed. The PL intensity increased with the annealing time and had a maximum at 2 hours annealing, and saturated or slightly diminished after 2 hours as shown in Figure 6. As PL intensity is known to be proportional to the total volume of Si nanocrystal,[20] this result indicated that the volume of nanocrystal increased until 2 hours and remained at a fixed

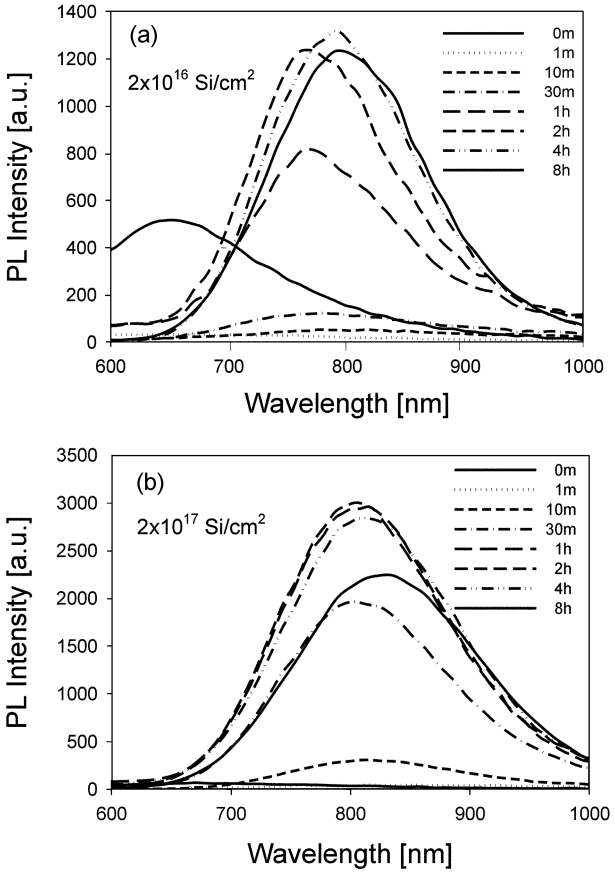

Figure 5. PL spectra of Si nanocrystals implanted with (a) 2×10^{16} Si/cm^2 and (b) 2×10^{17} Si/cm^2 dose and annealed at 1100 °C. Annealing time was varied 0 to 8 hours.

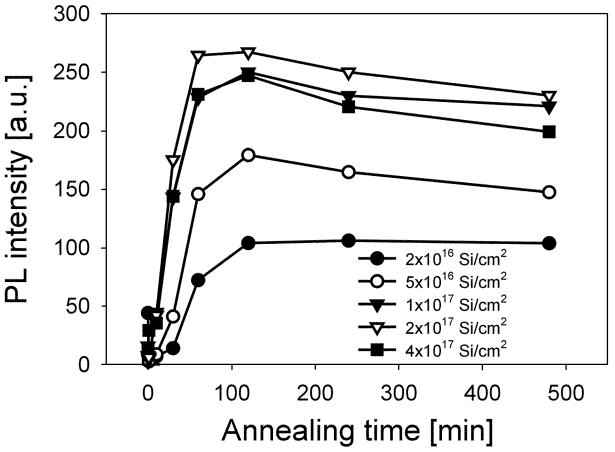

Figure 6. Peak emission intensity as a function of annealing time for implantation dose of 2×10^{16} Si/cm^2 and 4×10^{17} Si/cm^2.

value after 2 hours.

In the case of PL wavelength, the center of peak shifted to longer wavelength with annealing time as shown in Figure 7. When the annealing time increased over 2 hours, the red shift increased continuously although the intensity did not increase. It showed that the total volume fraction of precipitates was constant but the their size increased because of Ostwald ripening.[21]

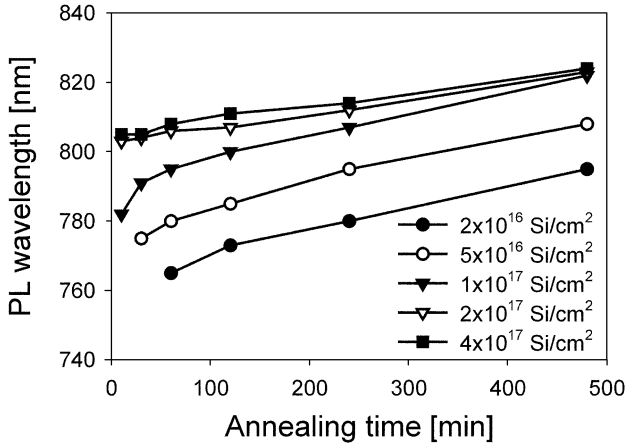

Figure 7. PL wavelength as a function of annealing time for implantation dose of 2×10^{16} Si/cm^2 and 4×10^{17} Si/cm^2.

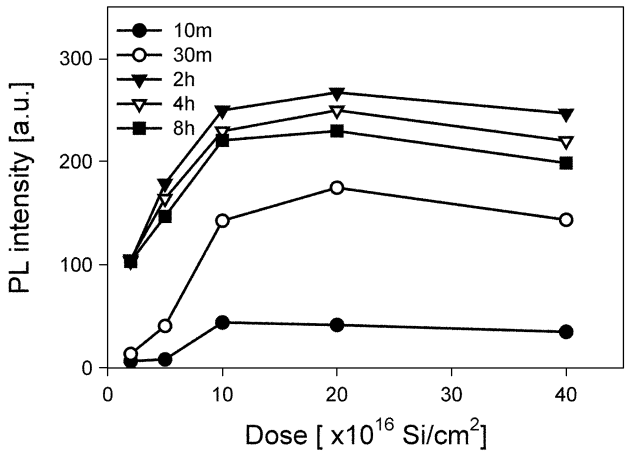

Figure 8. PL wavelength as a function of implantation dose for annealing time varied 10 to 480 minutes.

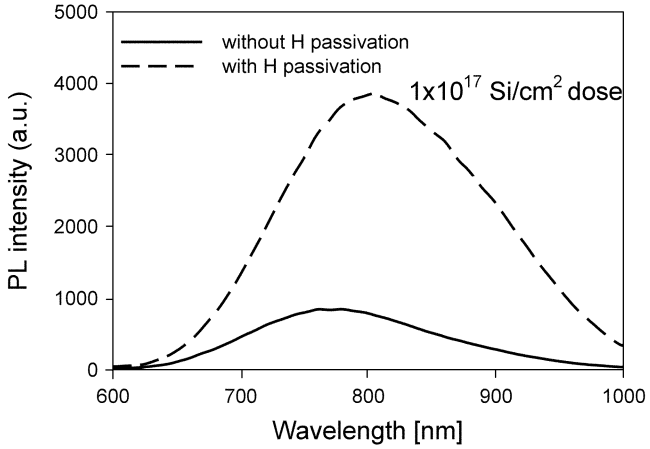

Figure 9. PL spectra of common Si nanocrystal and hydrogen passivated one.

PL intensity increased with dose and reached maximum at 2×10^{17} Si/cm^2 as shown in Figure 8. When the dose increased to 4×10^{17} Si/cm^2, size of nanocrystals increased so much so that the distance between surfaces of neighbor

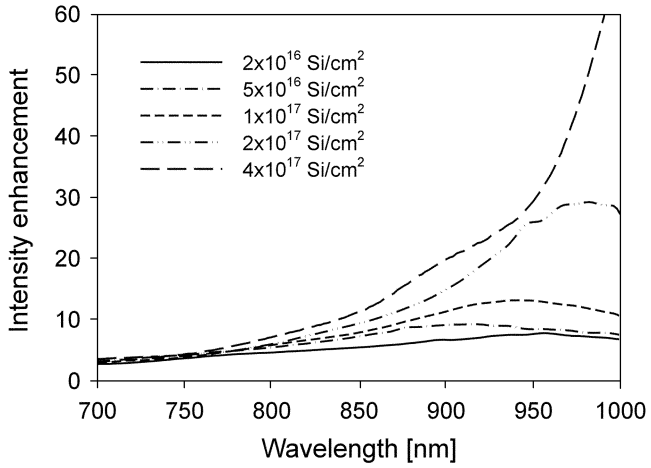

Figure 10. Passivation-induced enhancement of PL emission as a function of emission wavelength.

nanocrystals reduced less than 1 nm. And PL intensity decreased because quantum confinement was diminished by tunneling effect or interference between nanocrystals.[20] On the other side, the PL peak was shifted to red with Si dose because of the increase of the size.

Hydrogen passivated samples annealed at 500 °C for 1 hours in Ar + 4% H_2 gas showed stronger PL intensity than normal Si nanocrystal as shown in Figure 9. The enhancement by the hydrogen passivation increased monotonically with increasing wavelength (Fig. 10). Since longer wavelength emission is characteristic of larger nanocrystals, the data in Figure 10 are consistent with a disproportionate increase in the emission from lager nanocrystals following passivation. This implies that the passivation enhancement was induced by elimination of non-radiative defects on volume or surface area of nanocrystals because the number of defect is proportional to square or third order of nanocrystal diameter.[18]

Conclusion

The Si nanocrystals has been synthesized in fused silica plate by Si implantation and its formation was confirmed by HRTEM. A strong nanocrystal-based PL emission in 700-900 nm was observed. The size of nanocrystal increased with increasing annealing time and implantation dose. However, the total volume of nanocrystals got to constant after 2 hours annealing, and the intensity of PL decreased with extremely high dose because of the reduction of the gap between nanocrystals. A strong enhancement of PL intensity by H passivation was measured, and the enhancement is thought to be induced by the elimination of non-radiative defects on the volume or the surface of nanocrystals. In addition to this work, a time resolved PL decay will be measured to clear prove the enhancement mechanism. And non-thermal nucleation and low-energy implantation techniques will be tried to produce narrower size distribution than in the case of conventional implantation and thermal technique.

Acknowledgments. The Authors would like to appreciate Professor J. H. Shin at Korea Advanced Institute of Science and Technology for the helpful PL measurement. This work is supported by the Ministry of Science and Technology, Republic of Korea.

References

1. Song, H. Z.; Bao, X. M.; Li, N. S.; Zhang, J. Y. *J. Appl. Phys.* **1997**, *82*, 4028.
2. Shimizu-Iwayama, T.; Fujita, K.; Akai, M.; Nakao, S.; Saitoh, K. *J. Non Cryst. Solids* **1995**, *187*, 112.
3. Min, K. S.; Shcheglov, K. V.; Yang, C. M.; Atwater, H. A.; Brongersma, M. L.; Polman, A. *Appl. Phys. Lett.* **1996**, *69*, 2033.
4. Guha, S. J. *Appl. Phys.* **1998**, *84*, 5210.
5. Zharng, J. Y.; Bao, X. M.; Li, N. S.; Song, H. Z. *J. Appl. Phys.* **1998**, *83*, 3609.
6. Lee, C. W.; Kim, D. I.; Oh, M. K. *Bull. Korean Chem. Soc.* **1993**, *14*, 162.
7. Kim, D. I.; Lee, C. W. *Bull. Korean Chem. Soc.* **1995**, *16*, 1019.
8. Lan, A. D.; Liu, B. X.; Bai, X. D. *J. Appl. Phys.* **1997**, *82*, 5144.
9. Delerue, C.; Allan, G.; Lannoo, M. *Phys. Rev. B* **1993**, *48*, 11024.
10. Brongersma, M. L.; Polman, A.; Min, K. S.; Boer, E.; Tambo, T.; Atwater, H. A. *Appl. Phys. Lett.* **1998**, *72*, 2577.
11. Kanazawa, Y.; Kageyama, T.; Takeoka, S.; Fujii, M.; Hayashi, S.; Yamamoto, K. *Solid State Commun.* **1997**, *102*, 533.
12. Zhuravlev, K. S.; Gilinsky, A. M.; Kobitsky, A. Y. *Appl. Phys. Lett.* **1998**, *73*, 2962.
13. Kimura, K.; Iwasaki, S. *J. Appl. Phys.* **1998**, *83*, 1345.
14. Ma, S. K.; Lue, J. T. *Thin Solid Films* **1997**, *304*, 353.
15. Lan, A.; Liu, B. X.; Bai, X. D. *J. Appl. Phys.* **1994**, *82*, 378.
16. Min, K. S.; Shcheglove, K. V.; Yang, C. M.; Atwarter, H. A.; Brongersma, M. L.; Polman, A. *Appl. Phys. Lett.* **1998**, *72*, 4.
17. Withrow, S. P.; White, C. W.; Meldrum, A.; Budai, J. D.; Hembree Jr., D. M.; Barbour, J. C. *J. Appl. Phys.* **1999**, *86*, 1.
18. Cheylan, S.; Elliman, R. G. *Nucl. Instr. and Meth. in Phys. Res. B* **2001**, *175-177*, 422.
19. Shimizu-Iwayama, T.; Fujita, K.; Nakao, S.; Saitoh, K.; Fujita, T.; Itoh, N. *J. Appl. Phys.* **1994**, *75*, 7779.
20. Lopez, M.; Garrido, B.; Bonafos, C.; Perez-Rodriguez, A.; Morante, J. R.; Claverie, A. *Nucl. Instr. and Meth. in Phys. Res. B* **2001**, *178*, 89.
21. Bonafos, C.; Garrido, B.; Lopez, M.; Perez-Rodriguez, A.; Morante, J. R.; Ben Assayaf, G.; Claverie, A. *Mat. Sci. Eng. B* **1999**, *379*, 69.